Preparation of chitosan grafted graphite composite for sensitive detection of dopamine in biological samples

Selvakumar Palanisamy[1], Kokulnathan Thangavelu[1], Shen-Ming Chen*[1], P. Gnanaprakasam[2], Vijayalakshmi Velusamy[3], Xiao-Heng Liu[4**]

[1]Electroanalysis and Bioelectrochemistry Lab, Department of Chemical Engineering and Biotechnology, National Taipei University of Technology, No.1, Section 3, Chung-Hsiao East Road, Taipei 106, Taiwan (R.O.C).

[2]Department of Nanoscience and Nanotechnology, Karunya University, Coimbatore 64114, India

Corresponding author. Tel: +886 2270 17147; fax: +886 2270 25238.

[3]Division of Electrical and Electronic Engineering, School of Engineering, Manchester Metropolitan University, Manchester – M1 5GD, United Kingdom.

[4]Key Laboratory of Education Ministry for Soft Chemistry and Functional Materials, Nanjing University of Science and Technology, Nanjing 210094, China

Corresponding author. Tel: +886 2270 17147; fax: +886 2270 25238.

*E-mail address: smchen78@ms15.hinet.net (S.M. Chen); xhliu@mail.njust.edu.cn (X.H. Liu)

Abstract

The accurate detection of dopamine (DA) levels in biological samples such as human serum and urine samples are essential indicators in medical diagnostics. In this work, we describe the preparation of chitosan (CS) biopolymer grafted graphite (GR) composite for the sensitive and lower potential detection of DA in its sub micromolar levels. The composite modified electrode has been used for the detection of DA in biological samples such as human serum and urine samples. The GR-CS composite modified electrode shows 6 folds enhanced oxidation peak current response with low potential for the detection of DA than that of electrodes modified with bare, GR and CS discretely. Under optimum conditions, the fabricated GR-CS composite modified electrode shows the DPV response of DA in the linear response ranging from 0.03 to 20.06 µM. The detection limit and sensitivity of the sensor was estimated as 0.0045 µM and 6.06 µA μM^{-1} cm^{-2}.

Keywords: Graphite; chitosan; biopolymer; dopamine; electro-oxidation; differential pulse voltammetry.

1. Introduction

Over the past few decades, the development of biosensors and chemical sensors for the detection of neurotransmitters has received a great interest due to the vital role in the metabolic system of mammals (Pradhan et al., 2014; Jackowska and Krysinski, 2013). In particular, dopamine (DA) is a well-known inhibitory neurotransmitter and plays an important role in the central nervous system of the human (Nagatsu and Ichinose, 1999). In general, the DA level in the cerebrospinal fluid (CSF) is in the range between 0.5 to 25 nM (Suominen et al., 2013). Furthermore, the malfunctions of DA in CSF leads to many diseases such as Parkinsonism, schizophrenia, hypertension and pheochromocytoma (Ge et al., 2009). Therefore, the levels of DA in blood or urine are essential indicators in medical diagnostics for the diseases. To date, different analytical techniques have been utilized for the reliable determination of DA in biological fluids, such as liquid chromatography (Meng et al., 2000), capillary electrophoresis (Wey and Thormann, 2001), liquid chromatography coupled with UV detection (Ary and Rona, 2001), calorimetry (Secor and Glass, 2004), native fluorescence detection (Zhang et al., 2000) and electrochemical methods (Raj et al., 2003; Cabrita et al., 2005). However, the electrochemical methods are simple, rapid, cost-effective and efficient method for determination of DA than that of available traditional methods (Pandikumar et al., 2014).

In electrochemical DA sensors, the unmodified electrodes such as glassy carbon, graphite (GR) and screen printed carbon electrodes are not suitable for detection of DA, due to their poor selectivity, reproducibility, sensitivity and high overpotentials (Ghanbari and Hajheidari, 2015; Chen and Cha, 1999). Therefore, the carbon materials, metal oxide, metal alloy nanoparticles, redox and biopolymers modified electrodes have been widely used for the sensitive and selective detection of DA in lower overpotential (Pandikumar et al., 2014; Mao et al., 2015; Yan et al., 2015;

Li et al., 2015; Vasantha and Chen, 2006; Wang et al., 2006). On the other hand, chitosan (CS) is known non-toxic, highly biodegradable, naturally abundant linear carbohydrate biopolymer and widely used in the construction of electrochemical sensors and biosensors. Its various potential applications include, tissue engineering, artificial skin, burn treatment, wound healing, drug delivery, (Mertins and Dimova, 2013, 29; Rinaudo, 2006; Vusa et al., 2016). Recently, the CS functionalized graphene oxide and CS grafted graphene and carbon nanotubes have been used for the sensing of DA among its various applications (Shan et al., 2010; Demirkol and Timur, 2011; Liu et al., 2012; Wu et al., 2007; Niu et al., 2012). However, most of the reported DA sensors are based on CS with pristine graphene and or with carbon nanotubes, in which the composites are prepared by the direct sonication of graphene or carbon nanotubes in CS solution (Liu et al., 2012; Niu et al., 2012; Liu et al., 2014). More recently, we have reported DA sensor using the cyclodextrin grafted GR composite, and the resulting electrode has showed comparable performance over carbon nanomaterials modified electrodes for sensing of DA (Palanisamy et al., 2016). The motivation of the present work is to fabricate a simple, sensitive and reliable DA sensor using the CS grafted GR (GR-CS) composite modified electrode. The CS-GR composite can be easily prepared by sonication of GR and CS in acetic acid for 1 h at room temperature. Fewer reports have already reported for the preparation of CS grafted expanded GR (Jagiello et al., 2014; Demitri et al., 2015). However, for the first time we report a potential application of the GR-CS composite for the electrochemical sensing of DA.

In this work, a sensitive and selective DA sensor was developed based on GR-CS composite modified electrode for the first time. The GR-CS composite modified electrode shows an enhanced sensitivity with lower oxidation peak potential for DA than that of pristine GR and CS modified electrodes. In addition, the GR-CS modified electrode shows a superior performance

towards the oxidation of DA than graphene-CS composite, due to its strong intercalation of CS on exfoliated GR sheets. The selectivity and stability of the sensor were studied and discussed in detail. The practicability of the sensor also been evaluated in biological samples and discussed.

2. Experimental

2.1. Chemicals

Raw graphite, dopamine and chitosan (from crab shells, minimum 85% deacetylated) were obtained from Sigma. Uric acid, ascorbic acid and acetic acid were purchased from Aldrich. Graphene nanopowder (8 nm flakes, product number UR-GNAPHENE) was purchased from UniRegion Bio-Tech, Taiwan. Human blood serum sample was collected from valley biomedical, Taiwan product & services, Inc. This study was reviewed and approved by the ethics committee of Chang-Gung memorial hospital through the contract no. IRB101-5042A3 (Palanisamy et al., 2016). Human urine sample were collected from the two healthy persons and used for real sample analysis with their permission. The supporting electrolyte 0.05 M phosphate buffer pH 7 (PBS) was prepared by using 0.05 M Na_2HPO_4 and NaH_2PO_4 solutions in doubly distilled water and the pH were adjusted using 0.1 M H_2SO_4 and NaOH. All chemicals used in this study were of analytical grade and the solutions were prepared using double distilled water without any further purification.

2.2. Apparatus

Cyclic voltammetry (CV) and differential pulse voltammetry (DPV) measurements were performed by the CHI 750a electrochemical work station. Scanning electron microscopy (SEM) was performed using Hitachi S-3000 H electron microscope. Raman spectra were recorded using a Raman spectrometer (Dong Woo 500i, Korea) equipped with a charge-coupled detector. Fourier transform infrared spectroscopy (FT-IR) was carried out using the Thermo SCIENTIFIC Nicolet

iS10 instrument. Conventional three-electrode system was used for the electrochemical experiments, the glassy carbon electrode (GCE) with geometric surface area of 0.079 cm^2 was used as a working electrode, a saturated Ag/AgCl as a reference electrode and a platinum electrode as the auxiliary electrode. All electrochemical measurements were carried out at room temperature in N_2 atmosphere.

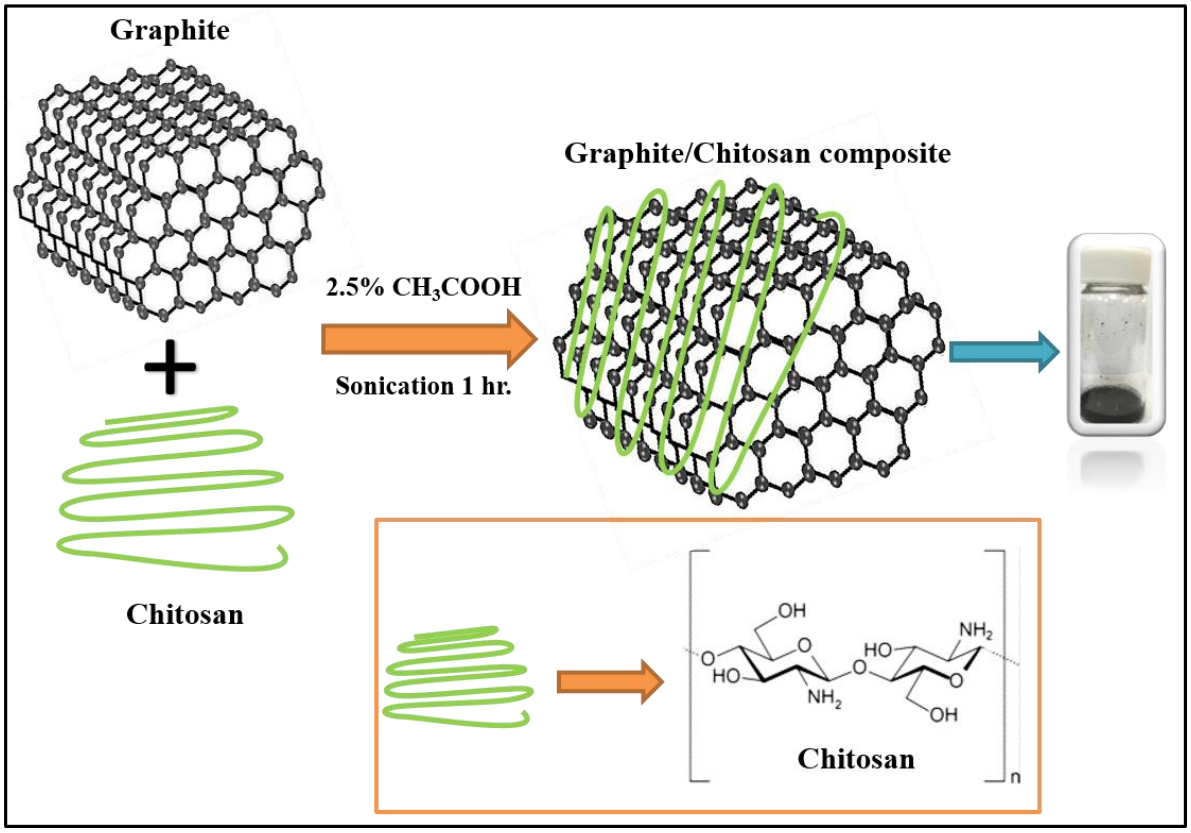

Scheme 1 Schematic representation of preparation of GR-CS composite.

2.3. Preparation of GR–CS composite

To prepare the CS-GR composite, first 15 mg of CS was dissolved in 3 mL of 2.5% acetic acid with the aid of ultra-sonication. Then, 10 mg GR (2:3 w/w, optimum) was added to the CS solution and continuously sonicated for 1 h at room temperature. The resulting GR-CS composite was centrifuged and dried in an air oven. The GR-CS composite was re-dispersed in ethanol and used for further electrochemical experiments. The preparation of CS-GR composite is shown in **Scheme**

1. For controls, GR solution was prepared by dispersing 10 mg of GR in dimethylformamide and CS solution was prepared by dissolving 15 mg of CS in 2.5% acetic acid. To prepare GR-CS modified electrode, about 9 µL (optimum) of GR-CS dispersion was drop coated onto pre-cleaned GCE and dried in room temperature. The GR and CS modified GCEs were independently prepared by drop coating of 9 µL of GR and CS on pre-cleaned GCE. For comparison with graphene-CS modified GCE, about 9 µL of the graphene-CS dispersion was drop casted on bare GCE and dried in an air oven. The graphene-CS dispersion was prepared by dispersing of 10 mg of graphene into the CS solution (2:3 w/w) with the help of ultrasonication for 1 h at room temperature.

3. Results and discussion

3.1. Characterization of GR-CS composite

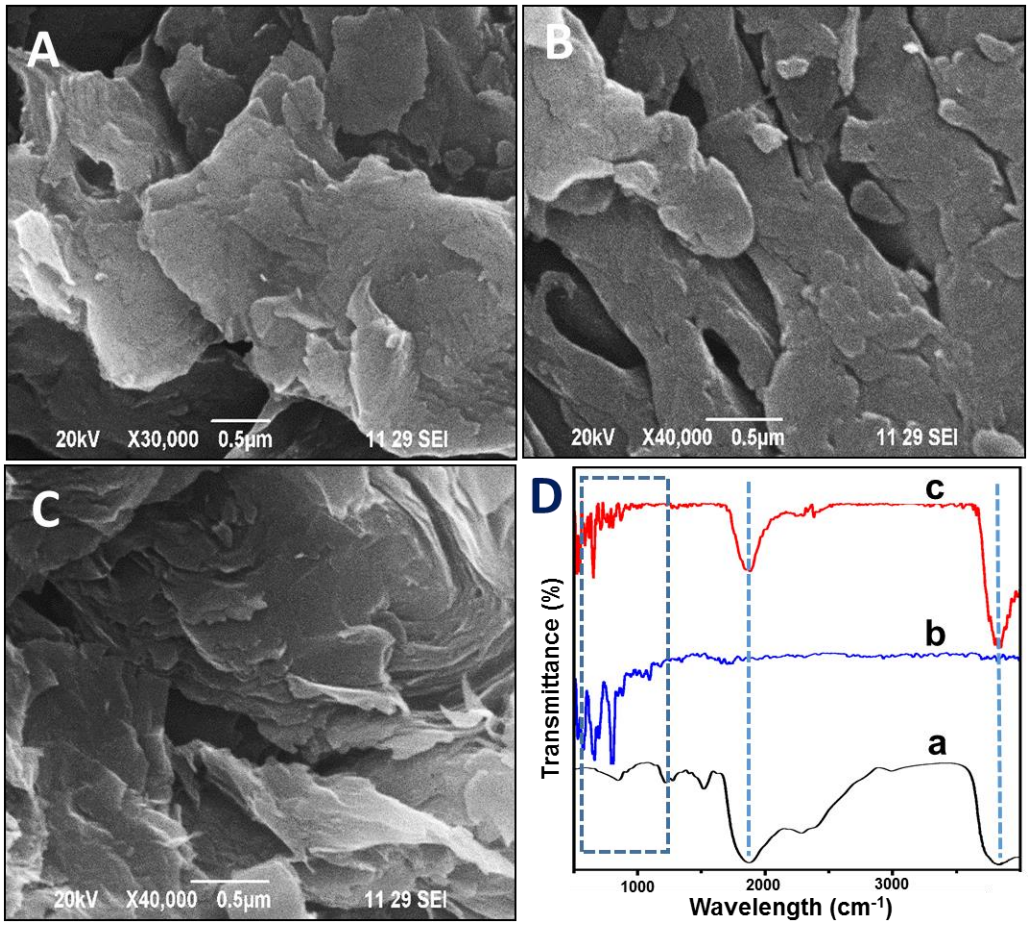

Fig. 1 SEM images of (A) pristine GR, B) CS and CS-GR (C). D) FT-IR spectra of CS (a), GR (b) and GR–CS (c).

The surface morphology of GR, CS and GR-CS composite was characterized by SEM. **Fig. 1** displays the SEM images of GR (A), CS (B) and GR-CS composite (C). The SEM image of GR reveals its typical flake sheet morphology with an association of micro graphitic sheets. On the other hand, the SEM image of CS reveals the uniform, thin and porous nature of CS. The SEM of GR-CS composite shows that the GR sheets were well separated and grafted with the highly porous thin film of CS. According to earlier studies, the CS macromolecule is enable to separate graphite layers and prevent the agglomeration of graphite (Jagiello et al., 2014). Typically, the electron pair on nitrogen in CS is in protonated form that enable the CS to strongly interact with graphite sheets, since graphite is known for electron donors (Jagiello et al., 2014). The similar phenomenon has been reported earlier for CS with graphene and GR. The formation of GR-CS composite was further confirmed by FTIR. **Fig. 1D** displays the FTIR spectra of CS (a), GR (b) and GR–CS (c). The FT-IR spectrum of CS depicts characteristic absorption band at 3811 and 3072 cm^{-1}, is attributed to the stretching vibrations of –OH. The absorption band at 1525, 1292 and 1114 cm^{-1}, attributed to stretching vibrations of C-O-N and C-O, respectively (Liu et al., 2006). In addition, two additional bands are observed at 1184 and 841 cm^{-1}, which is due to the glycosidic bonding of CS (Jagiello et al., 2014). On the other hand, the FTIR spectrum of GR show the bands at 1369 and 887 cm^{-1}, which is due to the –CH- bending vibration of GR. The absorption band of CS at 1525 cm^{-1} for C-O-N was disappeared when mixed with GR, and the absorption band at 1369 cm^{-1} for C-H stretch was shifted towards 1362 cm^{-1}. This is possibly due to the strong chemical interactions between the CS and GR and result into the exfoliation of GR sheets (Gedam et al.,

2015). In addition, the observed other absorption bands of GR-CS composite are consistent with the absorption bands of CS and GR, which confirms that the presence of CS in GR-CS composite.

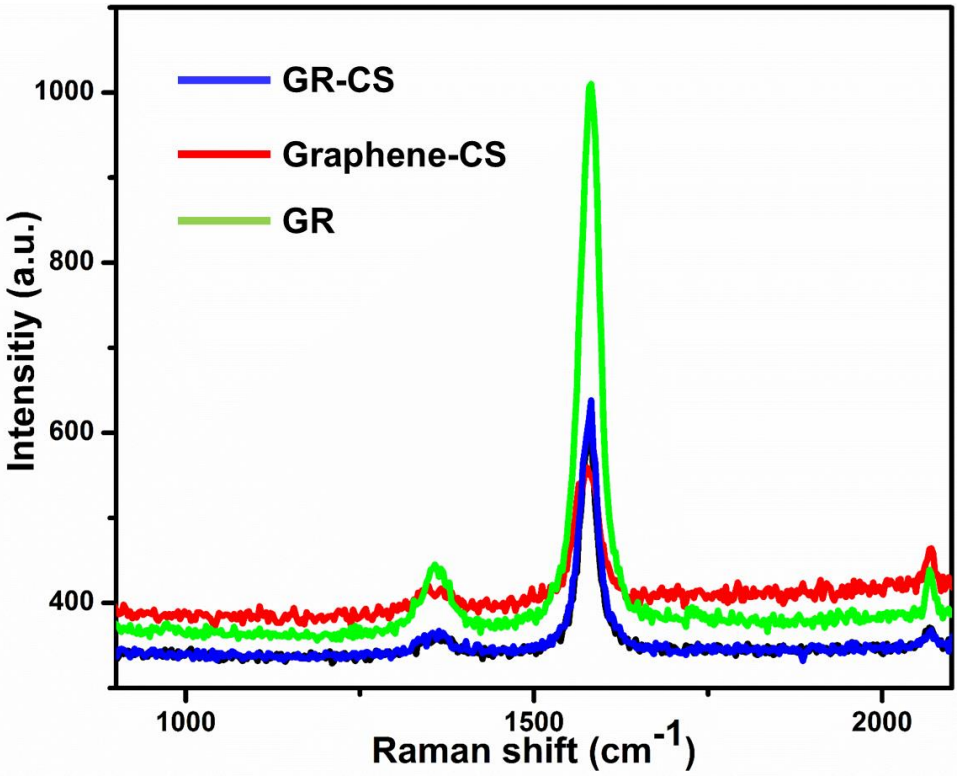

Fig. 2 A) Raman spectra of GR-CS (blue line), pristine GR (green line) and graphene-CS (red line).

Raman spectroscopy was further employed for characterization of GR and GR-CS composite and the results were compared with the Raman spectra of graphene-CS composite. **Fig. 2** shows the Raman spectra of GR (green profile), GR-CS (blue profile) and graphene-CS (red line). The G band is corresponding to the first-order scattering of the E2g mode in-phase vibration of the graphite lattice and D band is due to the out-of-plane breathing mode of the sp^2 atoms of graphite (Jagiello et al., 2014). The Raman spectrum of pure GR shows the weak D and strong G bands at 1354 and 1579 cm^{-1}. The D and G bands of CS grafted GR appears at 1363 and 1583 cm^{-1}, and the G band was greatly reduced after the introduction of CS on GR. In addition, the Raman

spectra of GR-CS composite is quite similar to the Raman spectra of graphene-CS composite. The result indicates that the successful transformation of GR by CS in GR-CS composite.

3.2. Electrochemical behavior of DA

CV was used to investigate the electrochemical behaviour of DA at GR-CS composite modified electrode. **Fig. 3A** shows the CV response of GR (a), bare (b), CS (c) and GR-CS (d) modified electrodes in 50 µM of DA containing PBS at a scan rate of 50 mV s^{-1}. The bare and GR modified electrodes exhibited a weak redox couple for DA and the oxidation peak potential (E_{pa}) of DA was observed at 0.507 and 0.360 V. The E_{pa} of DA was greatly deduced upon the introduction of CS on GCE, the E_{pa} of DA was observed at 0.298 V. In addition, the redox behaviour of DA is greatly enhanced when compared to the response observed in bare and GR modified electrodes. The result indicates the efficient electron transfer ability of CS towards the electrode surface. However, GR-CS composite modified electrode shows a pair of well-defined quasi-reversible redox peak for DA and the E_{pa} of DA was observed at 0.215 V. The observed E_{pa} of DA was 0.292, 0.145 and 0.083 V lower than that of GR, bare and CS modified electrodes. Furthermore, the oxidation peak current (I_{pa}) response of DA at GR-CS composite electrode was 4.2, 3.7 and 2.7 folds higher than the response observed in GR, bare and CS modified electrodes (**Fig. 3A inset**). The result indicates that GR-CS composite modified electrode has high electrocatalytic activity towards DA than that of other modified electrodes.

As reported earlier that the protonated form of CS in acidic acid solution could easily interact with the p electrons in sp^2 hybrid orbital of GR (Jagiello et al., 2014). In addition, the long chain of CS is more favourable to interact with each graphitic sheets in GR and result into exfoliation of GR. The exfoliated GR in GR-CS composite contains high number of basal planes per volume, while the amount of available edge plane remains the same (Figueiredo-Filho et al.,

2013). The large number of basal planes in GR-CS composite and result into the high surface area and high electrocatalytic activity towards DA. Furthermore, the distinct structure of CS plays an important role to prevent the accumulation of exfoliated GR in GR-CS composite (Jagiello et al., 2014). In order to further clarify the catalytic activity, the electrocatalytic behaviour of DA at GR/CS composite was compared with graphene-CS composite. **Fig. 3B** shows CV responses of graphene/CS (a) and GR-CS (b) modified electrodes in PBS containing 25 µM of DA in PBS at a scan rate of 50 mV s^{-1}. A well-defined quasi redox couple was observed for DA at graphene/CS composite modified electrode and the oxidation peak of DA was appeared at 0.284 V. However, the GR-CS modified electrode shows 2 folds enhanced oxidation peak current and lower overpotential (0.215 V) for detection of DA than that of graphene/CS composite modified electrode. It is evident from the result that the GR-CS composite has quite higher or similar electrocatalytic activity to graphene/CS modified electrode.

The CS grafted GR composite mostly exists in positive form when the pH was below 5 due to the protonation of $-NH_2$ group of CS (Jiang et al., 2004). While, the protonation of $-NH_2$ group is very low when the pH was more than 6.0, this is more favourable for H-bond interactions between CS and DA (Jiang et al., 2004). These are the possible reasons for enhanced electrochemical behavior and lower oxidation potential of DA at GR-CS composite. We have also investigated the electrochemical behaviour DA at graphene/CS composite and the results are compared with the response observed at GR-CS composite.

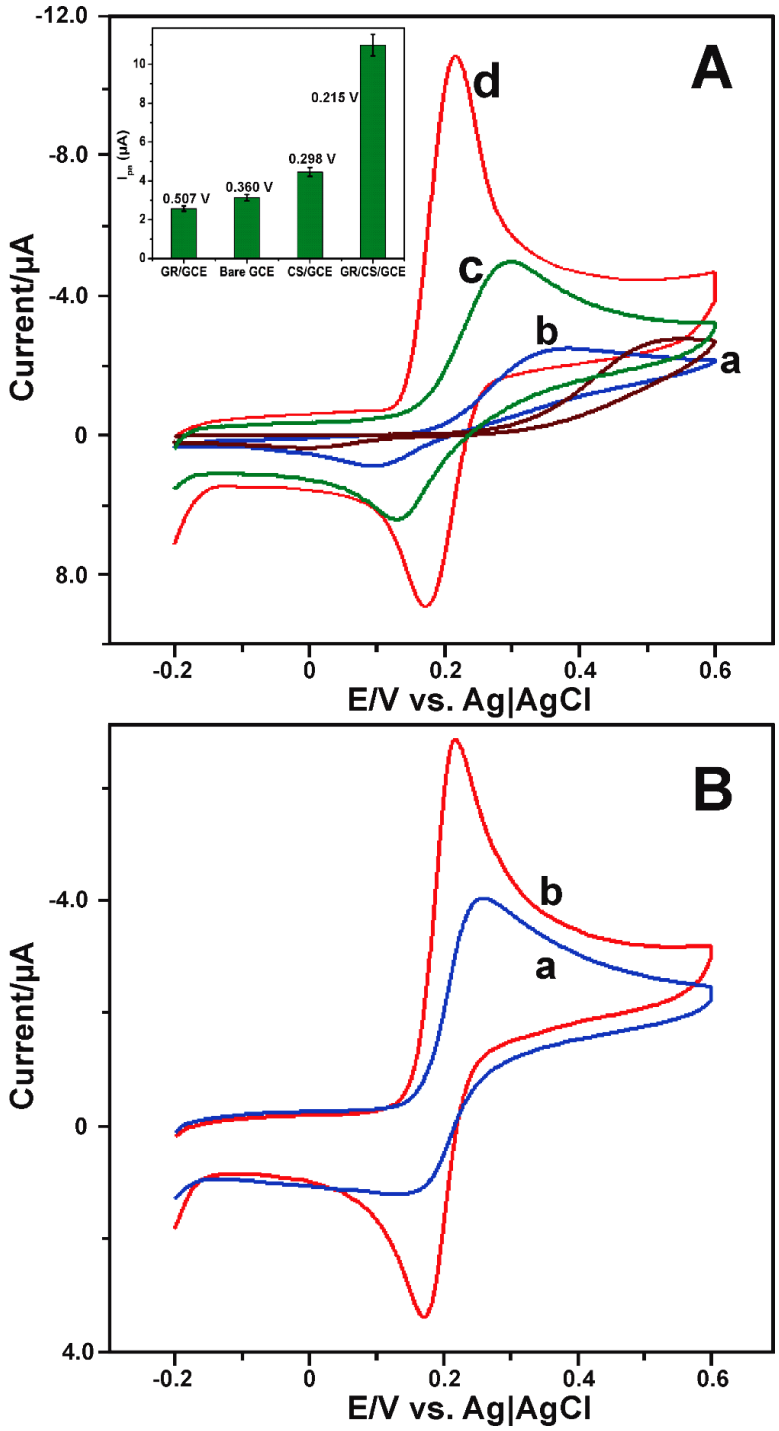

Fig. 3 A) CV response of the GR (a), bare (b), CS (c) and GR-CS (d) modified GCEs in 50 μM of DA containing PBS at a scan rate of 50 mV s^{-1}. Inset shows the I_{pa} and E_{pa} of DA vs. different modified electrodes. B) At the same conditions, CV response of the graphene-CS (a) and GR-CS (b) modified GCEs in 25 μM of DA containing PBS at a scan rate of 50 mV s^{-1}.

3.3. Optimization

The optimizations studies are more important and it may directly affect the electrochemical behaviour of DA. Hence, the optimization of GR, CS in GR-CS composite and drop coating amount of GR-CS composite towards the detection of 50 µM DA was investigated by CV. The experimental conditions are similar as of in **Fig. 3A**. The optimization results are shown in **Fig. S1A-C**. It can be seen from **Fig. S1A** and **B** that the high sensitivity of DA was observed for 2 and 3 wt% of GR and CS containing GR-CS composite. We have used GR and CS loading as 2 and 3 wt% for optimize the GR and CS. Hence, the 2 and 3 wt% of GR and CS was used for the preparation of GR-CS composite. In the same manner, 9 µL drop coated GR-CS composite modified electrode showed a maximum current response for DA than that of other drop coated electrodes (**Fig. S1C**). Hence, 9 µL drop coated GR-CS composite modified electrode was used as an optimum quantity for further electrochemical investigations.

3.4. Effect of scan rate and pH

The effect of scan rate on the electrochemical behaviour of 50 µM DA was investigated in PBS by CV. **Fig. 4A** shows the CV response of GR-CS modified electrode in 50 µM DA containing PBS at different scan rates from 10 to 300 mV s^{-1}. It can be seen that the I_{pa} and cathodic peak current (I_{pc}) of DA increases with increasing the scan rate from 10 to 300 mV s^{-1}.

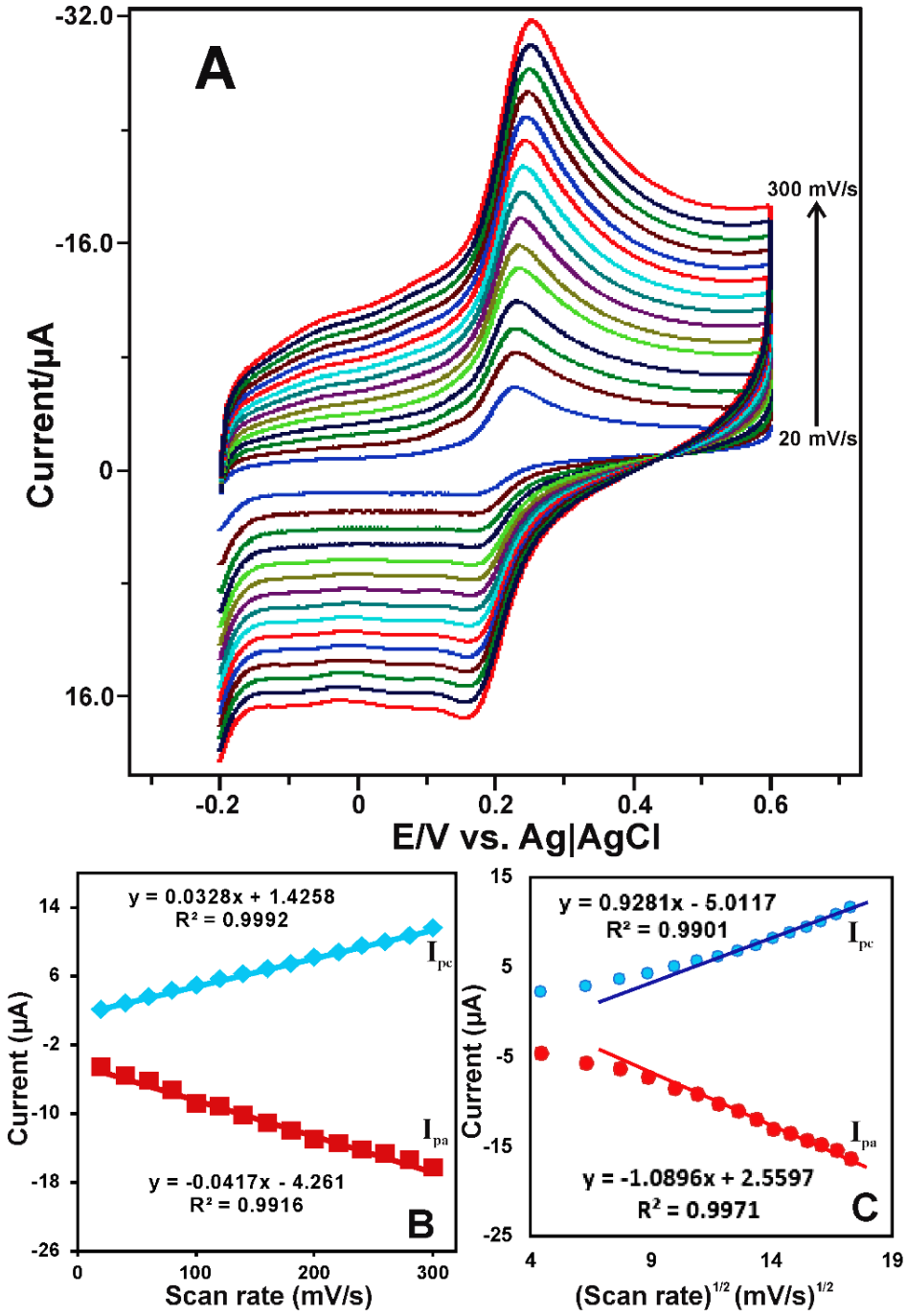

223

224 **Fig. 4** A) CV response obtained at GR-CS modified electrode in the presence of 50 µM DA

225 containing PBS at different scan rates from 10 to 300 mV/s. B) Linear dependence of scan rate vs.

226 I_{pa}. C) Linear plot of square root of scan rate vs. I_{pa}.

227 Furthermore, I_{pa} and I_{pc} had exhibited a linear relationship with a scan rate from 10 to 300

228 mV s^{-1} (**Fig. 4B**), which indicates that the electrochemical behaviour of DA is controlled by a

typical adsorption-controlled process. However, the (I_{pa}) and (I_{pc}) are linearly proportional to the square root of the scan rates from the scan rates from 120 to 300 mV s^{-1} (**Fig. 4C**), indicating that electrochemical behaviour of DA is a diffusion controlled process at higher scan rates. The above result confirms that the electrochemical behaviour of DA at GR-CS composite modified electrode is controlled by a mixed kinetic process.

The electrochemical redox behaviour of 75 µM DA was investigated using the GR-CS composite modified electrode in different pH solutions by CV. **Fig. S2A** shows the CV response of GR-CS composite modified electrode in different pH solutions (pH 3, 5, 7, 9 and 11) containing 75 µM of DA at a scan rate of 50 mV s^{-1}. A well-defined redox couple of DA was observed in each pH and the E_{pa} and reduction peak potential (E_{pc}) were shifted towards negative and positive direction upon increasing and decreasing the pH. Furthermore, the E_{pa} and E_{pc} of DA had a linear relationship between the pH from 3 to 11, as shown in **Fig. S2B**. The linear plot was derived against the formal potential ($E^{0'} = (E_{pa} + E_{pc})/2$) vs. pH and the slope value was found as 58.6 mV/pH with the correlation coefficient of 0.9854. The observed slope value is close to the theoretical slope value for an equal number of protons and electrons transferred electrochemical reaction, as reported previously (Palanisamy et al., 2016). The electrochemical mechanism of DA at carbon modified electrodes have been well demonstrated and the redox behaviour of DA at GR-CS composite involves two protons and two electrons coupled electrochemical reaction.

3.5. Determination of DA and selectivity of the biosensor

DPV was employed for the electrochemical determination of DA using the GR-CS composite modified electrode. **Fig. 5** shows the typical DPV response of the GR-CS composite modified electrode for the absence and presence of additions of different concentration of DA into the PBS. It can be seen that the GR-CS composite modified electrode did not show any apparent response

in the absence of DA. However, a sharp oxidation peak response was observed for the addition of DA from 0.05 to 22.06 µM. As shown in **Fig. 5 inset**, the GR-CS composite exhibited the response current of DA was linear over the concentration ranging from 0.03 to 20.06 µM with the correlation coefficient of 0.9958.

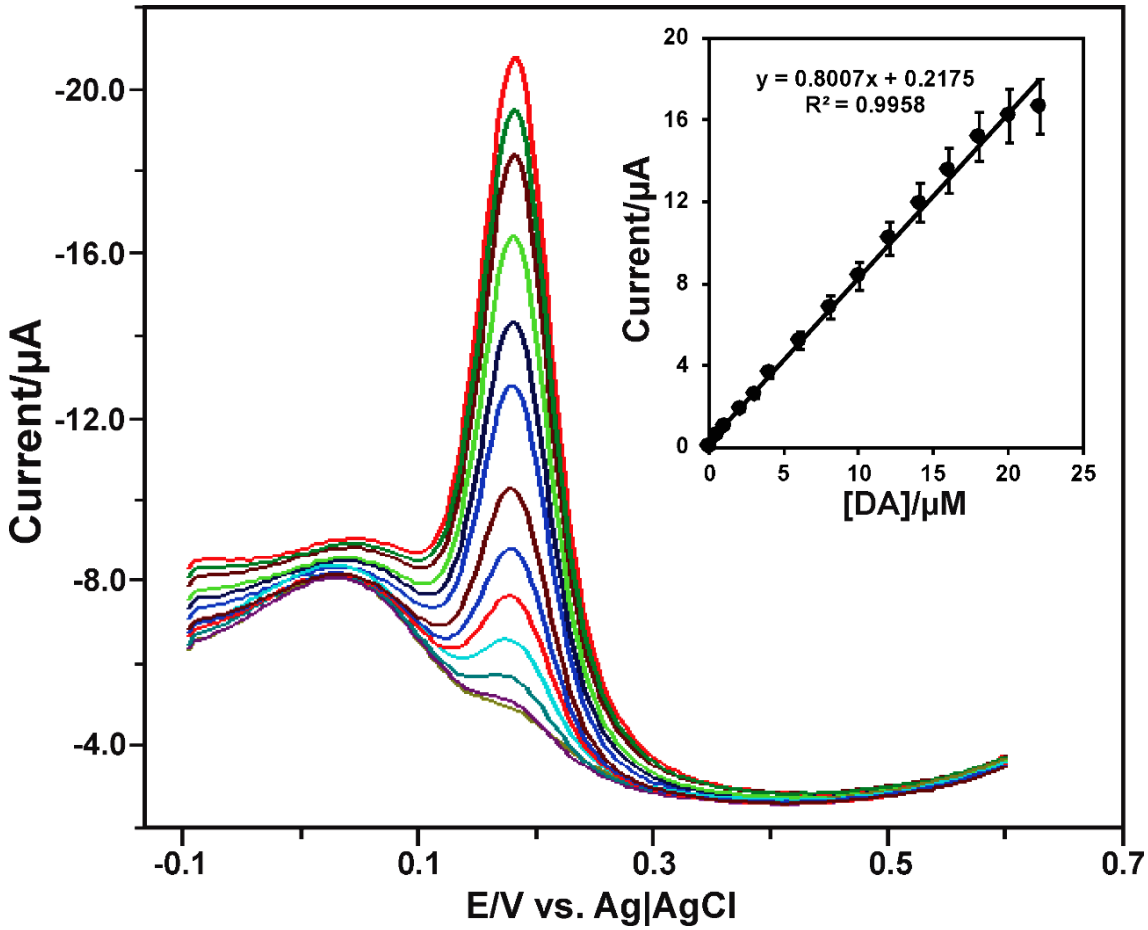

Fig. 5 A) DPV response of the GR-CS electrode for the additions of different concentration of DA into the PBS. Inset: Linear relationship of I_{pa} vs. [DA]. DPV conditions are: sampling width: 0.0167 s; pulse width: 0.05 s; pulse period: 0.2 s; amplitude: 0.05 V; quite time: 2 s.

The sensitivity of the developed sensor was estimated to be 6.06 $\mu A \mu M^{-1} cm^{-2}$ based on the slope value of the calibration plot. The GR-CS composite modified electrode active surface area was 0.12 cm^2. The limit of detection (LOD) was estimated as 0.0045 µM based on S/N=3. The

fabricated DA sensor exhibited low LOD for DA when compared to sulphonated CS (Vusa et al., 2016), CS entrapped graphene (Niu et al., 2012; Liu et al., 2014; 36. Weng et al., 2013; Han et al., 2010; Liu et al., 2011; Wang et al., 2013) and carbon nanotubes modified electrodes (Babaei et al., 2011), as shown in **Table ST1**. On the other hand, the obtained linear range of our sensor was quite narrow when compared to the previously reported modified electrodes for the detection of DA. We have also compared the analytical performance of the present DA sensor with previously reported tyrosinase based different DA sensors and the comparative results are shown in Table. S2. The comparison results clear that the fabricated DA sensor shows high sensitivity and comparable LOD and linear response for the detection of DA (Maciejewska et al., 2011; Zhou et al., 2007; Tsai et al., 2007; Tembe et al., 2008; Njagi et al., 2008; Min and Yoo, 2009; Njagi et al., Forzani et al., 1995; Hasebe et al., 1995; Cosnier et al., 1997; Pandey et al., 2001; Ve´drine et al., 2003; Tembe et al., 2006; Wang, et al., 2010). In addition, the developed DA sensor is less expensive and easy to prepare when compared with previously enzymatic and non-enzymatic DA sensors (Jackowska and Krysinski, 2013).

The selectivity of the modified electrode is much important for the detection of DA in the presence of potentially active compounds which are commonly present in biological samples, such as ascorbic acid (AA) and uric acid (UA). These compounds can potentially interfere the response of DA on the modified electrode due to their close oxidation potential with DA. Hence, the selectivity of GR-CS composite modified electrode towards the detection of DA was evaluated in the presence of AA and UA by DPV. The selectivity results are shown in **Fig. S3**. The experimental conditions and DPV working parameters are similar as of in **Fig. 5**. The GR-CS composite modified electrode shows a sharp oxidation peak at 0.194 V for the addition of 1 µM DA (a). while, 100 µM addition of AA (b) do not show any electrochemical response on the same potential

window. In addition, the response current and peak potential of DA was not affected in the presence of 100 µM AA, which clearly indicates that AA do not have cross reactivity with DA. On the other hand, the GR-CS composite modified electrode shows a tiny response at 0.384 V for the presence of 30 µM UA, and the response current of UA increases with the addition of 50, 100 and 200 µM of UA into the PBS. The oxidation peak current response of DA slightly affected in the presence of UA, while the peak potential of DA unaffected even in the presence of 200 µM UA. The protonation of $-NH_2$ group of CS in GR-CS composite is very weak when the pH was more than 6.0, hence the H-bonding is more favourable towards DA than that of interaction with UA and AA. This is the possible reasons for high selectivity of the GR-CS composite towards the detection of DA. The result clearly demonstrates the high selectivity of the fabricated DA sensor.

3.6. Determination of DA in biological samples

The practical ability of GR-CS composite modified electrode was evaluated by determination of DA in biological samples such as human blood serum and urine samples. The standard addition method was used for the determination of DA in human blood serum and urine samples. The DPV was used for the determination of DA and the experimental conditions are similar as of in **Fig. 5**. The human urine samples were diluted 10 times before the DPV measurements. The unknown concentration of DA was predetermined in DA containing spiked human serum and urine samples by DPV. Then, the known concentration of DA (2 µM) containing human blood serum and urine samples was spiked into the PBS. The obtained recovery results are summarized in **Table ST3**. The GR-CS composite modified electrode showed the average recovery of DA about 98.3 and 100.5 % DA in the human blood serum and urine samples. The result confirmed that the GR-CS composite modified electrode could be used for the reliable detection of DA in biological real samples.

The stability of the GR-CS composite modified electrode was examined periodically towards the detection of 50 µM of DA by CV for 6 days. The GR-CS composite modified electrode retains 93.6% of the initial current response of DA (figure not shown) after the storage (6 days) in PBS at 4 ˚C. The result indicates the good stability of the GR-CS composite modified electrode towards the detection of DA. The reproducibility and repeatability of the GR-CS composite modified electrode towards the detection of DA was evaluated by CV. The relative standard deviation (RSD) of 2.9% was found for 10 measurements of 50 µM DA by single GR-CS composite modified electrode. The five independently prepared GR-CS composite modified electrode shows the RSD of 4.3% for the detection of 50 µM DA. The results indicate that GR-CS composite modified electrode has good repeatability and reproducibility for the detection of DA.

4. Conclusions

We have reported a simple and reliable DA sensor using the GR-CS composite modified electrode for the first time. The modified electrode showed high catalytic activity and lower oxidation potential towards the detection of DA, which is attributed to the excellent conductivity and adsorption property of GR and CS. The as-prepared GR-CS composite modified electrode shows a high sensitivity, low LOD, appropriate response range and satisfactory stability for the detection of DA. The GR-CS composite modified electrode has many practical advantages over the reported nanomaterials modified electrodes for the detection of DA, such as cost-effective, highly reproducible and can be prepared in short period of time (1 h). The fabricated electrode showed high selectivity towards DA in the presence of excess addition of AA and UA. The good recovery of DA in human serum and in urine samples authenticates that the fabricated GR-CS composite electrode is well suitable for the detection DA for biological and medicinal applications.

Acknowledgments

This project was supported by the Ministry of Science and Technology, Taiwan (Republic of China).

References

Ary, K., & Rona, K. 2001. LC determination of morphine and morphine glucuronides in human plasma by coulometric and UV detection, J. Pharm. Biomed. Anal., 26, 179–187.

Babaei, A., Babazadeh. M., & Momeni, H.M. 2011. A sensor for simultaneous determination of dopamine and morphine in biological samples using a multi-walled carbon nanotube/chitosan composite modified glassy carbon electrode, Int. J. Electrochem. Sci., 6,1382–1395.

Cabrita, J.F., Abrantes, L.M., & Viana, A.S. 2005. N-Hydroxysuccinimide-terminated self-assembled monolayers on gold for biomolecules immobilization, Electrochim. Acta., 50, 2117–2124.

Chen, J., & Cha, C.S. 1999. Detection of dopamine in the presence of a large excess of ascorbic acid by using the powder microelectrode technique, J. Electroanal. Chem., 463, 93–99.

Cosnier, S., Innocent, C., Allien, L., Poitry, S., & Tsacopoulos, M. 1997. An electrochemical method for making enzyme microsensors. application to the detection of dopamine and glutamate, Anal. Chem., 69, 968–971.

Demirkol, D.O., & Timur, S. 2011. Chitosan matrices modified with carbon nanotubes for use in mediated microbial biosensing, Microchim. Acta.,173, 537–542.

Demitri, C., Moscatello, A., Giuri, A., Raucci, M.G., & Corcione, C.E. 2015. Preparation and characterization of eg-chitosan nanocomposites via direct exfoliation: a green methodology, Polymers., 7, 2584–2594.

356 Figueiredo-Filho, L.C.S., Brownson, D.A.C., Mingot, M.G., Iniesta, J., Fatibello-Filho, O., &
357 Banks, C.E. 2013. Exploring the electrochemical performance of graphitic paste electrodes:
358 graphene vs. graphite, Analyst., 138, 6354–6364.
359 Forzani, E.S., Rivas, G.A., & Solis, V.M. 1995. Amperometric determination of dopamine on
360 an enzymatically modified carbon paste electrode, J. Electroanal. Chem., 382, 33–40.
361 Ge, B., Tan, Y., Xie, Q., Ma, M., & Yao, S. 2009. Preparation of chitosan–dopamine-multiwalled
362 carbon nanotubes nanocomposite for electrocatalytic oxidation and sensitive
363 electroanalysis of NADH, Sen. Actuators B., 137, 547–554.
364 Gedam, A.H., Dongre, R.S., & Bansiwal, A.K. 2015. Synthesis and characterization of graphite
365 doped chitosan composite for batch adsorption of lead (II) ions from aqueous solution, Adv.
366 Mater. Lett., 6, 59–67.
367 Ghanbari, K., & Hajheidari, N. 2015. ZnO–CuxO/polypyrrole nanocomposite modified
368 electrode for simultaneous determination of ascorbic acid, dopamine, and uric acid, Anal.
369 Biochem., 473, 53–62.
370 Han, D., Han, T., Shan, C.S., Ivaska, & A., Niua, L. 2010. Simultaneous determination of
371 ascorbic acid, dopamine and uric acid with chitosan-graphene modified electrode,
372 Electroanalysis., 22, 2001–2008.
373 Hasebe, Y., Hirano, T., & Uchiyama, S. 1995. Determination of catecholamines and uric acid in
374 biological fluids without pretreatment, using chemically amplified biosensors, Sens.
375 Actuators, B., 24-25, 94–97.
376 Jackowska, K., & Krysinski. P. 2013. New trends in the electrochemical sensing of dopamine,
377 Anal. Bioanal. Chem., 405, 3753–3771.

Jagiello, J., Judek, J., Zdrojek, M.M., Aksienionek, M., & Lipinska, L. 2014. Production of graphene composite by direct graphite exfoliation with chitosan, Mater. Chem. Phy, 148, 507–511.

Jiang, L., Liu, C., Jiang, L., Peng, Z., & Lu, G. 2004. A chitosan-multiwall carbon nanotube modified electrode for simultaneous detection of dopamine and ascorbic acid, Anal. sci., 20, 1055–1059.

Li, B., Zhou, Y., Wu, W., Liu, M., Mei, S., Zhou, Y., & Jing, T. 2015. Highly selective and sensitive determination of dopamine by the novel molecularly imprinted poly (nicotinamide)/CuO nanoparticles modified electrode, Biosens. Bioelectron., 67, 121–128.

Liu, B., Lian, H.T., Yin, J.F., & Sun, X.Y. 2012. Dopamine molecularly imprinted electrochemical sensor based on graphene–chitosan composite, Electrochim. Acta., 75, 108–114.

Liu, C., Zhang, J., Yifeng, E., Yue, J., Chen, L., & Li, D. 2014. One-pot synthesis of graphene–chitosan nanocomposite modified carbon paste electrode for selective determination of dopamine, Electron. J. Biotechnol., 17, 183–188.

Liu, H., Bao, J., Du, Y., Zhou, X., & Kennedy, J.F. 2006. Hydration energy of the 1, 4-bonds of chitosan and their breakdown by ultrasonic treatment, Carbohydr. Polym., 64, 553–559.

Liu. X., Peng, Y., Qua, X., Ai, S., Han, R., & Zhu, X. 2011. Multi-walled carbon nanotube chitosan/poly(amidoamine)/DNA nanocomposite modified gold electrode for determination of dopamine and uric acid under coexistence of ascorbic acid, J. Electroanal. Chem., 654, 72–78.

399 Maciejewska, J., Pisareka, K., Bartosiewicza, I., Krysinski, P., Jackowska, K., & Biegunski, A.
400 T. 2011. Selective detection of dopamine on poly (indole-5-carboxylic acid)/tyrosinase
401 Electrode, Electrochim. Acta., 56, 3700-3706.
402 Mao, H., Liang, J., Zhang, H., Pei, Q., Liu, D., Wu, S., Zhang, Y., & Song, X.M. 2015. Poly
403 (ionic liquids) functionalized polypyrrole/graphene oxide nanosheets for electrochemical
404 sensor to detect dopamine in the presence of ascorbic acid, Biosens. Bioelectron., 70, 289–
405 298.
406 Meng, Q. C., Cepeda, M.C., Kramer, T., Zou, H., Matoka, D.J., & Farrar, J. 2000. High-
407 performance liquid chromatographic determination of morphine and its 3-and 6-
408 glucuronide metabolites by two-step solid-phase extraction, J. Chromatogr. B., 742, 115–
409 123.
410 Mertins, O., & Dimova, R. 2013. Insights on the interactions of chitosan with phospholipid
411 vesicles. part i: effect of polymer deprotonation, Langmuir., 29, 14545−14551.
412 Min, K., & Yoo. Y.J. 2009. Amperometric detection of dopamine based on tyrosinase–SWNTs–
413 Ppy composite electrode, Talanta., 80, 1007–1011.
414 Nagatsu, T., & Ichinose, H. 1999. Molecular biology of catecholamine-related enzymes in
415 relation to Parkinson's disease, Cell. Mol. Neurobiol., 19, 57–66.
416 Niu, X., Yang, W., Guo, H., Ren, J., Yang, F., & Gao, J. 2012. A novel and simple strategy for
417 simultaneous determination of dopamine, uric acid and ascorbic acid based on the stacked
418 graphene platelet nanofibers/ionic liquids/chitosan modified electrode, Talanta, 99, 984–
419 988.

Njagi, J., Chernov, M.M., Leiter, J.C., & Andreescu, S. 2010. Amperometric detection of dopamine in vivo with an enzyme based carbon fiber microbiosensor, Anal. Chem., 82, 989–996.

Njagi, J., Ispas, C., & Andreescu, S. 2008. Mixed ceria-based metal oxides biosensor for operation in oxygen restrictive environments, Anal. Chem., 80, 7266–7274.

Palanisamy, S., Sakthinathan, S., Chen, S.M., Thirumalraj, B., Wu, T.H., Lou, B.S., & Liu, X. 2016. Preparation of β-cyclodextrin entrapped graphite composite for sensitive detection of dopamine, Carbohydr.Polym., 135, 267–273.

Pandey, P.C., Upadhyay, S., Tiwari, I., Singh. G & Tripathi, V.S. 2001. A novel ferrocene encapsulated palladium–linked ormosil-based electrocatalytic dopamine sensor, Sens. Actuators, B.,75, 48–55.

Pandikumar, B., How, G.T.S., See, T.P., Omar, F.S., Jayabal, S., Kamali, K.Z., Yusoff, N., Jamil, A., Ramaraj, R., John, S.A., Lim, H.N., & Huang, N.M. 2014. Graphene and its nanocomposite material based electrochemical sensor platform for dopamine, RSC Adv., 4, 63296–63323.

Pradhan, T., Jung, H.S., Jang, J.H., Kim, T.W., Kang, C., & Kim, J.S. 2014. Chemical sensing of neurotransmitters, Chem. Soc. Rev., 43, 4684–4713.

Raj, C. R., Okajima, T., & Ohsaka, T.J. 2003. Gold nanoparticle arrays for the voltammetric sensing of dopamine, Electroanal. Chem., 543, 127–133.

Rinaudo, M. 2006. Chitin and chitosan: properties and applications, Prog. Polym. Sci., 31,603–632.

Secor, K.E., & Glass, T.E. 2004. Selective amine recognition: development of a chemosensor for dopamine and norepinephrine, Org. Lett., 6, 3727–3730.

443 Shan, C., Yang, H., Han, D., Zhang, Q., Ivaska, A., & Niu, L. 2010. Graphene/AuNPs/chitosan
444 nanocomposites film for glucose biosensing, Biosens.Bioelectron., 25, 1070–1074.
445 Suominen, T., Uutela, P., Ketola, R.A., Bergquist, T., Hillered, L., Finel, M., Zhang, H., Laakso,
446 A., & Kostiainen, R. 2013. Determination of serotonin and dopamine metabolites in human
447 brain microdialysis and cerebrospinal fluid samples by UPLC-MS/MS: discovery of intact
448 glucuronide and sulfate conjugates, PLoS One., 8, e68007.
449 Tembe, S., Karve, M., Inamdar, S., Haram, S., Melo, J., & D'Souza, S.F. 2006. Development of
450 electrochemical biosensor based on tyrosinase immobilized in composite biopolymeric
451 film, Anal. Biochem., 349, 72–77.
452 Tembe, S., Kubal, B.S., Karve, M., & D'Souza, S.F. 2008. Glutaraldehyde activated eggshell
453 membrane for immobilization of tyrosinase from amorphophallus companulatus:
454 Application in construction of electrochemical biosensor for dopamine, Anal. Chim. Acta.,
455 612, 212–217.
456 Tsai, Y.C., & Chiu, C.C. 2007. Amperometric biosensors based on multiwalled carbon nanotube-
457 nafion-tyrosinase nanobiocomposites for the determination of phenolic compounds, Sens.
458 Actuators, B., 125, 10–16.
459 Vasantha, V.S., & Chen, S.M. 2006. Electrocatalysis and simultaneous detection of dopamine
460 and ascorbic acid using poly (3, 4-ethylenedioxy) thiophene film modified electrodes, J.
461 Electroanal. Chem., 592, 77–87.
462 Ve´drine, C., Fabiano, S., & Minh, C.T. 2003. Amperometric tyrosinase based biosensor using
463 an electrogenerated polythiophene film as an entrapment support, Talanta., 59, 535–544.

Vusa, C.S.R., Manju, V., Aneesh, K., Berchmans, S., & Palaniappan, A. 2016. Tailored interfacial architecture of chitosan modified glassy carbon electrodes facilitating selective, nanomolar detection of dopamine, RSC Adv., 6, 4818–4825.

Wang, H.S., Li, T.H., Jia, W.L., & Xu, H.Y. 2006. Highly selective and sensitive determination of dopamine using a nafion/carbon nanotubes coated poly(3-methylthiophene) modified electrode, Biosens. Bioelectron., 22, 664–669.

Wang, X., Wu, M., Tang, W., Zhu, Y., Wang, L., Wang, Q., He, P., & Fang, Y. 2013. Simultaneous electrochemical determination of ascorbic acid, dopamine and uric acid using a palladium nanoparticle/graphene/chitosan modified electrode, J. Electroanal. Chem., 695, 10–16.

Wang, Y., Zhang, X., Chen, Y., Xu, H., Tan, Y., & Wang, S. 2010. Detection of dopamine based on tyrosinase-Fe_3O_4 nanoparticles-chitosan nanocomposite biosensor, Am. J. Biomed. Sci., 2(3), 209–216.

Weng, X., Cao, Q., Liang, L., Chen, J., You, C., Ruan, Y., Lin, H., & Wu, L. 2013. Simultaneous determination of dopamine and uric acid using layer-by-layer graphene and chitosan assembled multilayer films, Talanta., 117, 359–365.

Wey, A.B., & Thormann, W. 2001. Capillary electrophoresis–electrospray ionization ion trap mass spectrometry for analysis and confirmation testing of morphine and related compounds in urine, J. Chromatogr. A., 916, 225–238.

Wu. Z., Feng. W., Feng. Y., Liu. Q, Xu. X, Sekino. T, Fujii. A., & Ozaki, M. 2007. Preparation and characterization of chitosan-grafted multiwalled carbon nanotubes and their electrochemical properties, Carbon., 45, 1212–1218.

Yan, Y., Liu, Q., Du, X., Qian, J., Mao, H., & Wang, K. 2015. Visible light photoelectrochemical sensor for ultrasensitive determination of dopamine based on synergistic effect of graphene quantum dots and TiO_2 nanoparticles, Anal. Chim. Acta., 853, 258–264.

Zhang, X.X., Li, J., Gao, J., Sun, L., & Chang, W.B. 2000. Determination of morphine by capillary electrophoresis immunoassay in thermally reversible hydrogel-modified buffer and laser-induced fluorescence detection, J. Chromatogr. A, 895, 1–7.

Zhou, Y.L., Tian, R.H., & Zhi. J.F. 2007. Amperometric biosensor based on tyrosinase immobilized on a boron-doped diamond electrode, Biosens. Bioelectron., 22, 822–828.

Research highlights and TOC